

Distributions of in-situ parameters, dissolved (in)organic carbon, and nutrients in the water column and pore waters of Arctic fjords (Western Spitsbergen) during a melting season

Seyed Reza Saghravani^{1,*}, Michael Ernst Böttcher^{2,3,4}, Wei-Li Hong^{5,6}, Karol Kuliński¹, Aivo Lepland⁷,
5 Arunima Sen^{8,9}, Beata Szymczycha¹

¹Marine Chemistry and Biochemistry Department, Institute of Oceanology Polish Academy of Sciences (IOPAN),
Powstańców Warszawy 55, Sopot 81-712, Poland

10 ²Geochemistry and Isotope Biogeochemistry, Leibniz Institute for Baltic Sea Research (IOW), Seestrasse 15, D-18119
Warnemünde, Germany

³Marine Geochemistry, University of Greifswald, D-17489 Greifswald, Germany

⁴Maritime Systems, Interdisciplinary Faculty, University of Rostock, D-18059 Rostock, Germany

⁵Department of Geological Sciences, Stockholm University, Svante Arrhenius väg 8, Stockholm 11418, Sweden

⁶Baltic Sea Centre, Stockholm University, Universitetsvägen 10 A, 10691, Stockholm, Sweden

15 ⁷Geological Survey of Norway, Leiv Eirikssons vei 39, 7040, Trondheim, Norway

⁸Department of Arctic Biology, University Centre in Svalbard, N-9171, Longyearbyen, Norway

⁹Faculty of Bioscience and Aquaculture, Nord University, 8049, Bodø, Norway

*Correspondence to: Seyed Reza Saghravani (reza@iopan.pl)

20

Abstract. A nutrient distribution such as phosphate (PO_4^{3-}), ammonium (NH_4^+), nitrate (NO_3^-), dissolved silica (Si), total dissolved nitrogen (TN), dissolved organic nitrogen (DON) together with dissolved organic carbon (DOC) and inorganic carbon (DIC), was investigated during a high melting season in 2021 in the western Spitsbergen fjords (Hornsund, Isfjorden, Kongsfjorden and Krossfjorden). Both the water column and the pore water were investigated for nutrients and dissolved
25 carbon distribution and gradients. The water column concentrations of most measured parameters, such as PO_4^{3-} , NH_4^+ , NO_3^- , Si, and DIC showed significant changes among fjords and water masses. In addition, pore water gradients of PO_4^{3-} , NH_4^+ , NO_3^- , Si, DIC and DOC revealed significant variability between fjords and are likely substantial sources of the investigated elements for the water column. The reported dataset reflects differences in hydrography and biogeochemical ecosystem functions of the investigated western Spitsbergen fjords and may form the base for further modelling of physical oceanographic
30 and biogeochemical processes within these fjords. All data discussed in this communication are stored in the Zenodo online repository; <https://doi.org/10.5281/zenodo.11237340> (Szymczycha et al., 2024).

1 Introduction

35 The Arctic is facing significant and rapid transformations due to Arctic amplification accelerating climate change in the region
(Dunse et al., 2021). Warming of climate causes changes in oceanic and atmospheric circulation patterns, permafrost
degradation, a decrease in the thickness and extent of sea ice, as well as a shrinkage of glaciers (IPCC, 2019; Dunse et al.,
2021). Freshwater released from glacial meltwater runoff or frontal ablation and accompanied fluxes of solutes, is a significant
40 factor that changes the hydrographic pattern and biogeochemistry of water masses, which in turn affects the biological
productivity in the ocean and fjords (Hopwood et al., 2016, 2020).

Many studies have investigated the biogeochemistry of nutrients in the Barents Sea and Arctic region (Henley et al., 2020;
Gundersen et al., 2022; Tuerena et al., 2022). Substantial efforts have been made in existing Arctic monitoring programmes,
research initiatives, and scientific projects to describe, explain and predict environmental changes due to diverse pressures for
the Arctic ecosystem (Townhill et al., 2022). Studies indicate that net primary production in open Arctic waters is mainly
45 sustained by the upwelling of nutrients and light availability (Henley et al., 2020; Stroeve et al., 2021) while nitrogen is
considered to be the key limiting nutrient in the Arctic Ocean (Mills et al. 2018; Ko et al. 2020). In addition, Henley et al.
(2020) indicated that, with ongoing sea ice losses due to Atlantification, the expected shift from more Arctic-like ice-impacted
conditions to more Atlantic-like ice-free conditions is projected to increase nutrient availability and the duration of the
vegetation period in the Arctic shelf region.

50 Arctic fjords have not gained similar attention and investigations were usually focused on individual fjord systems (Codispoti
et al., 2013; Henley et al., 2020; Kim et al., 2022; Pogojeva et al., 2022). Spatially wide studies of fjords and investigations
focusing on the hydrography and biogeochemical functioning of the Arctic shelf seafloor are still lacking. To address the
existing knowledge gaps, we studied the water masses, and pore waters, together with their biogeochemical composition in
the western Spitsbergen fjords. The selected area is an excellent research site for investigating the effects of both rapidly
55 occurring climate change and varied levels of Atlantification, as different fjords are under the diverse impact of the East
Spitsbergen Current bringing cold Arctic Water (ArW) and the West Spitsbergen Current carrying warmer and more saline
Atlantic Water (AtW). This was also our motivation to release this macronutrient dataset, which we believe may constitute a
biogeochemical reference for other experimental and modelling research in the region.

60 2 Materials and methods

2.1 Study area description

The west coast of the Svalbard archipelago (76 - 80°N) consists of different fjords and sub-fjords (Fig. 1). All investigated
fjords (Hornsund, Isfjorden, Kongsfjorden and Krossfjorden) are influenced by the East Spitsbergen Current carrying cold
65 ArW from the Barents Sea and the West Spitsbergen Current with warmer and more saline AtW from the Norwegian Sea
(Promińska et al., 2018) (Fig. 1). When AtW mixes with ArW, the warmer Transformed Atlantic Water (TAW) forms (Cottier
et al., 2005). Surface water (SW) is formed locally from glacial melt and river runoff, and occupies the surface layer of the

fjord. Intermediate Water (IW) forms as a result of mixing AtW or TAW with overlying fresher SW. Local Water (LW) and Winter Cooled Water (WCW) forms usually during autumn and winter (Cottier et al., 2005; Hop et al., 2006; Cantoni et al., 2020) in depressions within the inner fjords.

Hornsund is located at the southern end of Spitsbergen, and is about 30km long and 15km wide. The fjord is divided into the main basin and inner basin (Brepollen) by a shallow sill located in the centre of the fjord (Błaszczuk et al., 2019). The average depth is approximately 90m, while the deepest reaches 250m (Moskalik et al., 2014). Sediments consist of mud and sandy mud, laminated mud, homogeneous to bioturbated mud and sandy gravel (Drewnik et al., 2016). Freshwater discharge to the fjord was estimated to be approximately 1.8km³ annually (Weslawski et al., 1991), mainly due to glacier melting (64%) with the fastest retreating rate in Svalbard (with an average rate between 100 and >200m·yr⁻¹ (Grabiec et al., 2018). Other freshwater sources, such as frontal ablation and river runoff, influence primarily the upper water column (Zaborska et al., 2020). Hornsund exhibits high nutrient enrichment and experiences a strong influence from the ArW and colder coastal water (Włodarska-Kowalczyk et al., 1998). These conditions contribute to greater productivity in Hornsund compared to the warmer and saline fjords (Santos-Garcia et al., 2022).

Isfjorden stands as the largest fjord system on Spitsbergen having about 100km length from the mouth to the head and up to 425m deep. Isfjorden has several subfjords and bays. Studies conducted in Isfjorden have provided evidence of the significant impact of freshwater on the water column (McGovern et al., 2020; Finne et al., 2022). Seasonal stratification has been responsible for the retention of terrestrial carbon and nutrients within the euphotic zone and a decrease in vertical mixing during the most productive season (McGovern et al., 2020; Finne et al., 2022). The enhanced freshwater input contributes to the overall nutrient loading in the system, affecting the biogeochemical processes and ecosystem functioning.

Kongsfjorden is about 20km long and up to 10km wide with an orientation from south-east to north-west (Promińska et al., 2017). The depth at the mouth of the fjord is about 360m and decreases towards the inner part where it does not exceeds 100m (Svendsen et al., 2002). Kongsfjorden has remained sea ice-free since 2011, invoking profound biogeochemical transformations (Hop and Wiencke, 2019; Pavlova et al., 2019). Unlike other Arctic fjords, it experiences a distinct influence from the intrusion of warm and saline waters (Hodal et al., 2012). The inflow of AtW and ArW from one side and glacier meltwater from another (Halbach et al., 2019) lead to both amplified nutrients and carbon cycling, enhanced net primary productivity and oxygen depletion in deeper waters (Santos-Garcia et al., 2022).

Krossfjorden exhibits a north-east to south-west orientation, stretching approximately 30km in length and reaching widths from 3km to 6km. The total volume of Krossfjorden 25km³ and a maximum depth of 373m (Svendsen et al., 1992). Krossfjorden, characterized by a colder spring and less intrusion of AtW, shares similar conditions to the inner part of Kongsfjorden. However, it experiences a shorter period of glacier retreat compared to Kongsfjorden (Gamboa-Sojo et al., 2022). Studies on chlorophyll and other pigment distribution in surface sediments suggest that Krossfjorden is more productive than Kongsfjorden (Singh and Krishnan, 2019).

2.2 Sampling and Analyses

Sampling was carried out from 25th July to 20th August 2021 on board the r/v Oceania belonging to the Institute of Oceanology, Polish Academy of Sciences (IOPAN). A towed CTD profiling system (rosette) equipped with 10L Niskin bottles was used to collect water samples from 3 to 5 depths at each location (selected based on salinity and oxygen profiles). Temperature (T), salinity (S), and oxygen (O₂) concentration were measured in situ using a Sea-Bird Scientific SBE 911 Plus CTD profiler equipped with oxygen module SBE 43 (calibrated prior to the cruise). The accuracy of T, S and O₂ equals to ±0.002 °C, ±1% and ±0.015%, respectively. The results of averaged data for 0.5m intervals are presented in the database. Temperature and salinity from layers where discrete samples were collected were used for an oceanographic classification of water masses.

2.2.1 Seawater sampling

10ml of seawater was filtered (cellulose acetate filters with a pore size of 0.45µm), frozen in a pre-cleaned high-density polyethylene bottle and stored at -20°C for further nutrient analysis. The seawater for DIC analysis was transferred into the pre-cleaned 250ml glass bottle and poisoned with 100µl saturated HgCl₂. 20 ml of seawater for DOC and TN analysis were filtered through pre-combusted 0.45µm MN GF-5 filters and transferred into the pre-combusted glass bottle and acidified to pH~2 with HCl_{conc.} to stop mineralization and remove carbonates.

2.2.2 Pore water sampling

GEMAX and Nemisto gravity corers were used to collect up to approximately 40 cm long sediment cores. However, the retrieval of the cores in some locations was not possible due to the consolidated seafloor. Additionally, the pore water extracted from some sediment cores was insufficient to perform all analyses. Pore water was extracted from sediments through pre-drilled holes in the core liners via Rhizon® samplers (Rhizosphere, diameter of 2.5mm, and mean pore size of 0.15µm) directly after extracting the cores. Up to 5ml of pore water was frozen in a pre-cleaned high-density polyethylene bottle and stored at -20°C for further nutrient analysis and approximately 2ml of pore water was kept in PE vials for further Cl⁻ analysis. 12ml of pore water was transferred into the pre-combusted glass bottle and poisoned with 50µl saturated HgCl₂ for further DIC, DOC and TN analysis. Seawater pH was measured with a WTW Multi 3400i Field Multi-Parameter meter that yielded an accuracy of ±0.1. The pH results are given for a reference temperature of 25°C.

2.2.3 Chemical Analyses

Nutrient concentrations were determined using a SEAL AA500 AutoAnalyzer (Seal Analytical) applying standard photometric methods (Grasshof et al., 1983). Quality control consists of repeated measurements of two different CRMs (QC3179, Sigma Aldrich and HAMIL, Environment Canada). Method detection limits are 0.33µmol L⁻¹ for nitrate (NO₃⁻), 0.27µmol L⁻¹ for NH₄⁺, 0.1µmol L⁻¹ for phosphate (PO₄³⁻), 0.3 µmol L⁻¹ for dissolved silicates (Si). The accuracy of NO₃⁻, NH₄⁺, PO₄³⁻ and Si measurements was 98.8%, 98.8%, 99.0% and 100.1%, respectively, while the precision was 0.01µmol L⁻¹, 0.02µmol L⁻¹, 0.01µmol L⁻¹ and 0.03µmol L⁻¹, respectively. Chloride (Cl⁻) was determined by titration (Mohr's Method) with precision of 0.1mmol L⁻¹. The DIC analyses were carried out based on sample acidification with Apollo SciTech's AS-C6L DIC Analyzer

135 equipped with the laser-based CO₂ detector (LI-7815, Li-Cor, USA). The accuracy for DIC measurements was ensured by
using certified reference materials (CRMs, batches no. #190 and #195) from A.G. Dickson (Scripps Institution of
Oceanography, USA) and the precision was obtained from triplicate measurements of individual samples and was not worse
than $\pm 3 \mu\text{mol L}^{-1}$ with an average recovery 99.0%. The DOC and TN analyses were done in a TOC-L analyzer (Shimadzu)
140 L⁻¹; the accuracy was determined by repeated measurements of the certified reference materials (CRMs) provided by the D.
Hansell Laboratory (University of Miami, USA), and the recovery was 99%. The accuracy of the TN measurements was
guaranteed by using the same CRMs used to determine DOC, average recovery was 97%. DON was determined by subtracting
the sum of NO₃⁻ and NH₄⁺ from TN results.

145 **2.3 Statistics and data analysis**

All statistical analyses were carried out using Statistica (Statistica 13) while the evaluation of the statistical significance was
made using the Kruskal-Wallis test. Figure 1 was prepared in the Svalbard Map. Temperature-Salinity (TS) diagrams were
made using Python programming language, while box plots were made by means of Statistica.

150 **3 Data description**

3.1 Water masses distribution

Different water masses were distinguished within the investigated fjords (Fig.2; Szymczycha et al., 2024). The classification
was done based on Cottier et al., (2005), Nilsen et al., (2008) and Promińska et al., (2018) separately for each fjord ([Table 1](#)).
All the identified water masses align with those previously recognized in Arctic regions (Rudels et al., 2000) with some
155 interesting differences found between the fjords. In Hornsund SW, ArW, WCW and IW were found. In Isfjorden SW, ArW,
IW, LW and TAW occurred. In Kongsfjorden and Krossfjorden IW, TAW and AT were observed. It is worth noticing that
Hornsund did not show any impact by TAW and AtW.

3.2 Water column data

160 The distribution of T, S, pH, O₂, NO₃⁻, NH₄⁺, PO₄³⁻, Si, DIC, DOC, TN and DON in summer 2021 in western Spitsbergen
fjords was investigated. The obtained results were divided into the fjords such as Hornsund (marked blue), Isfjorden (marked
grey), Kongsfjorden (marked red) and Krossfjorden (marked yellow) (Fig.3; Szymczycha et al., 2024). In all studied fjords
similar trends were observed such as decrease of T, pH and increase of S, NO₃⁻, NH₄⁺, PO₄³⁻, Si, DIC, and TN with depth,
while O₂, DOC and DON were variable with depth and did not show any pattern. To show the variability of measured
165 parameters between fjords and separate the most freshened surface waters, the results were divided into the surface water layer
(the uppermost layer up to 5m: based on salinity and temperature) and the bottom water (the lowermost layer in the water
column) in each fjord (Fig. 4). Generally, the temperature of the surface water was warmer than that of the bottom water and
shows a significant difference between the fjords (p=0.00005) with the highest in Isfjorden and the coldest in Kongsfjorden.

The bottom water temperature was similar in all fjords ($p=0.1732$), however only in Hornsund reached negative values. Salinity was much higher in bottom water (median >34) than in surface water (median <33.5) and did not show significant differences between fjords ($p<0.05$) in both surface and bottom water. The pH of the surface water was high (median >7.8) and did not vary significantly between the fjords, while the pH of the bottom water was lower than the pH of the surface water and differed significantly between the fjords ($p=0.0109$). The median concentration of O_2 in both surface and bottom water was comparable and ranged from $308.8\mu\text{mol L}^{-1}$ to $333.8\mu\text{mol L}^{-1}$. NO_3^- , NH_4^+ , PO_4^{3-} and DIC showed a significant difference in the median concentration between surface and bottom water and significantly varied between fjords in both water types ($p<0.05$). Si showed a pattern similar to that of the other nutrients; however, in Isfjorden no significant change was observed between the surface and bottom. DOC did not change substantially between fjords and between water types. Interestingly, DOC, TN and DON showed similar behavior in all fjords.

180 3.3 Biogeochemistry of the water masses

In general, all fjord systems are transition zones between land and sea, resulting in complex and dynamic environments (Schlegel et al., 2023). The West Spitsbergen Fjords are highly stratified (Fig. 3) and provide a pathway for the exchange of heat, salt, nutrients, and dissolved carbon between near-glacier waters and adjacent coastal regions (Hopwood et al., 2020). These coastal regions are additionally under varying influence of the East Spitsbergen Current and the West Spitsbergen Current, which brings cold ArW and warmer and more saline AtW, respectively. It is worth mentioning that the West Spitsbergen Current, in addition to transporting the majority of heat, also transports carbon and plankton supply (Menze et al., 2020). However, the West Spitsbergen Current along its way up to Kongsfjorden is being depleted in nutrients (Smoła, 2017), and therefore, the influence on Kongsfjorden will be different from that of the Isfjorden. Thus, understanding the biogeochemical processes in the fjords and characterizing the differences among them is not possible without a detailed understanding of the water circulation. To characterize the distribution of T, S, pH, O_2 , NO_3^- , NH_4^+ , PO_4^{3-} , Si, DIC, DOC, TN and DON in the investigated fjords, we used the Kruskal-Wallis test to characterize the differences in the concentrations of these constituents between different water masses within and between investigated fjords (Fig. 5). The p-value is presented only if there was a significant difference in the median concentration of the parameter considered between the investigated fjords. SW, ArW and IW were characterized with different compositions of most of the measured parameters such as NO_3^- , NH_4^+ , PO_4^{3-} , Si, and DIC between fjords. Besides NH_4^+ , Arctic Water is enriched in nutrients and DIC in Hornsund in comparison to Isfjorden. However, the LW, which was only observed in Isfjorden, was characterized by the highest concentration of NO_3^- , PO_4^{3-} , Si, and DIC between all water masses.

3.4 Pore water data

200 The distribution and gradients of Cl^- , NO_3^- , NH_4^+ , PO_4^{3-} , Si, DIC, DOC in pore waters in the investigated fjords are presented in Figure 6 (Szymczycha et al., 2024). Generally, Cl^- , NH_4^+ , PO_4^{3-} , Si, and DIC increased with depth and NO_3^- and DOC decreased with depth. PO_4^{3-} decreased in every fjord except Isfjorden. To highlight the potential of the pore waters dataset for

further assessment and interpretation by data users, the concentrations of investigated parameters in pore water up to 5 cm and the concentrations in bottom water were compared in Figure 7.

205 The median concentrations of Cl^- in pore water did not differ significantly among fjords and were comparable to those of bottom water, apart from Isfjorden, where the median concentrations of Cl^- in pore water were smaller than those of bottom water. In all fjords, NO_3^- was higher in bottom water compared to pore water, while NH_4^+ , PO_4^{3-} , Si, and DIC were significantly higher in pore water in comparison to bottom water. The median concentration of NO_3^- , NH_4^+ , PO_4^{3-} , Si, and DIC was significantly different in both water types ($p < 0.05$). The median concentration of DOC was slightly higher in pore water than
210 in bottom water. However, it is worth noticing that the concentration ranges for all of the measured parameters differ between and within the investigated fjords.

4. Applications of the dataset

This dataset is beneficial for the broad scientific community that is interested in arctic physical oceanography and marine
215 biogeochemistry. In addition, the presented dataset provided evidence for the spatial distribution of nutrients and the dissolved carbon species in the investigated Arctic fjords. The data are made accessible as base for a wider dissemination that will lead to an enhanced understanding and new scientific insights into the nutrient cycles in the Arctic fjords. Possible applications may include: 1) being a reference and allowing comparison of the current measurements of the nutrients and dissolved carbon distribution in both the water column and sediments in the same region with future studies, 2) the determination of C:N:P:Si
220 ratios in different water masses and their comparison between fjords, as an assessment of the environmental controls and limiting factors for the primary production, and 3) parameterization, validation, and improvement of existing and future biogeochemical models.

5. Data Availability

225 All data described in this paper are stored in the Zenodo online repository (<https://doi.org/10.5281/zenodo.11237340> (Szymczycha et al., 2024)).

230

235

6. List of tables:

240 Table 1. Salinity and temperature of various water masses in fjords. The classification was done based on Cottier et al., (2005), Nilsen et al., (2008) and Promińska et al., (2018) separately for each fjord.

	<u>Hornsund</u> <u>(Nilsen et al., 2008)</u>		<u>Isfjorden</u> <u>(Nilsen et al., 2008)</u>		<u>Kongsfjorden-Krossfjorden</u> <u>(Cottier et al. 2005)</u>	
	<u>Temperature (°C)</u>	<u>Salinity</u>	<u>Temperature (°C)</u>	<u>Salinity</u>	<u>Temperature (°C)</u>	<u>Salinity</u>
<u>Arctic Water (ArW)</u>	<u>-1.5 > T > 2</u>	<u>34 < S < 34.5*</u>	<u>-1.5 > T > 1</u>	<u>34.4 < S < 34.8</u>	<u>-1.5 > T > 1</u>	<u>34.30 < S < 34.80</u>
<u>Atlantic Water (AW)</u>	<u>T > 3</u>	<u>S > 34.9</u>	<u>T > 3</u>	<u>S > 34.9</u>	<u>T > 3</u>	<u>S > 34.65</u>
<u>Intermediate Water (IW)</u>	<u>T > 1</u>	<u>34 < S < 34.7</u>	<u>T > 1</u>	<u>34 < S < 34.7</u>	<u>T > 1</u>	<u>34.00 < S < 34.65</u>
<u>Local water (LW)</u>	<u>T < 1</u>		<u>T < 1</u>		<u>-1.5 > T > 1</u>	<u>34.30 < S < 34.85</u>
<u>Surface Water (SW)</u>	<u>T > 1</u>	<u>34 < S</u>	<u>T > 1</u>	<u>34 < S</u>	<u>T > 1</u>	<u>S < 34</u>
<u>Transformed Atlantic Water (TAW)</u>	<u>T > 1</u>	<u>34.7 < S < 34.9</u>	<u>T > 1</u>	<u>S > 34.7</u>	<u>1 > T > 3</u>	<u>S > 34.65</u>
<u>Winter Cooled Water (WCW)</u>	<u>T < -0.5</u>	<u>S > 34.4</u>	<u>T < -0.5</u>	<u>S > 34.74</u>	<u>T < - 0.5</u>	<u>34.40 < S < 35</u>

*Promińska et al. (2018)

245

250

255

260 7. List of figures:

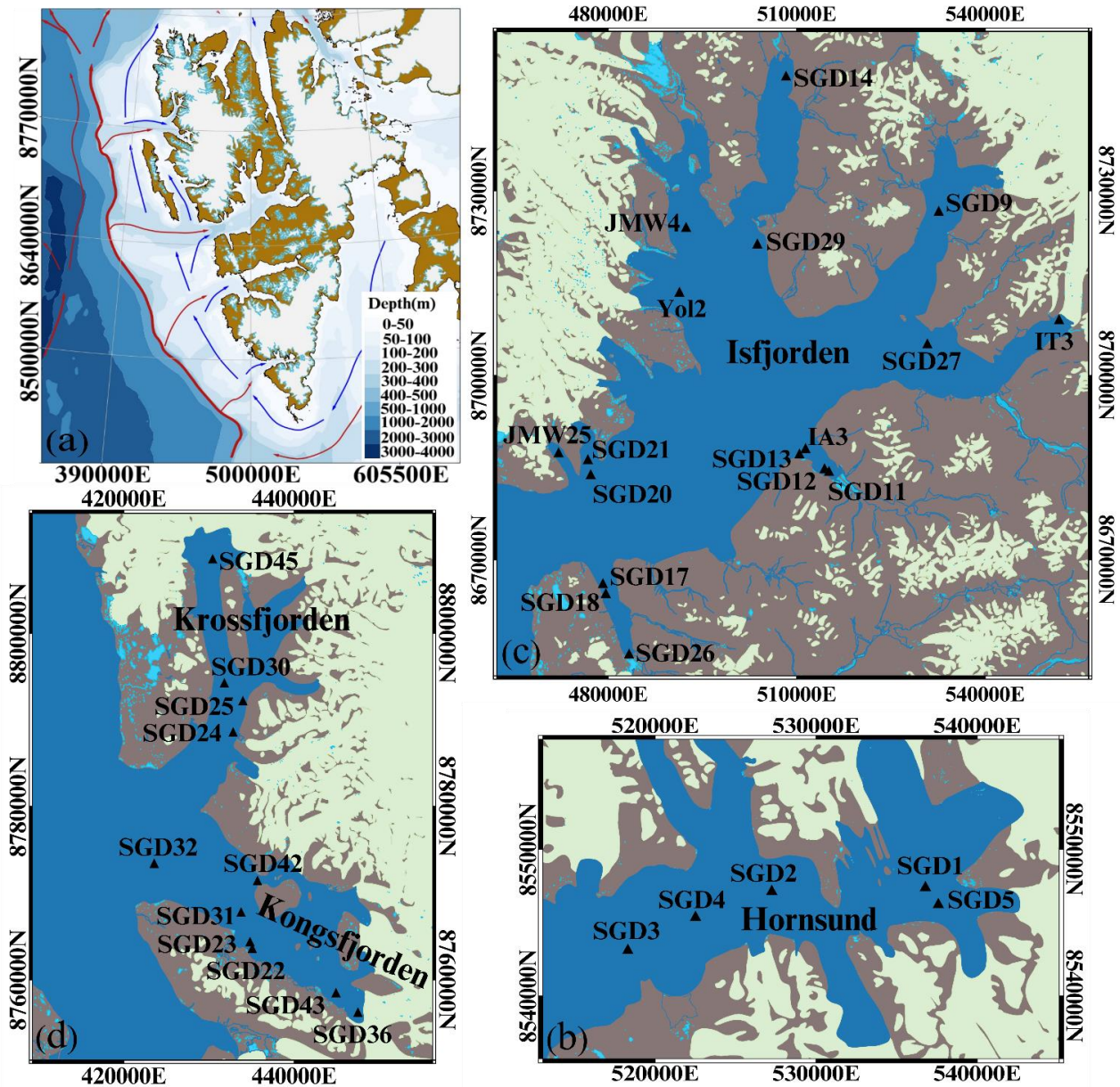


Fig.1 a) Study Area including the general map of Spitsbergen, highlighting the depths of the fjords and the surrounding Svalbard shelf (a). The warm West Spitsbergen Current and cold East Spitsbergen Current are indicated by red and blue arrows, respectively (Vihtakari, 2022, 2020). Study sites located in b) Hornsund, c) Isfjorden, and d) Kongsfjorden and Krossfjorden are presented as black triangles.

265

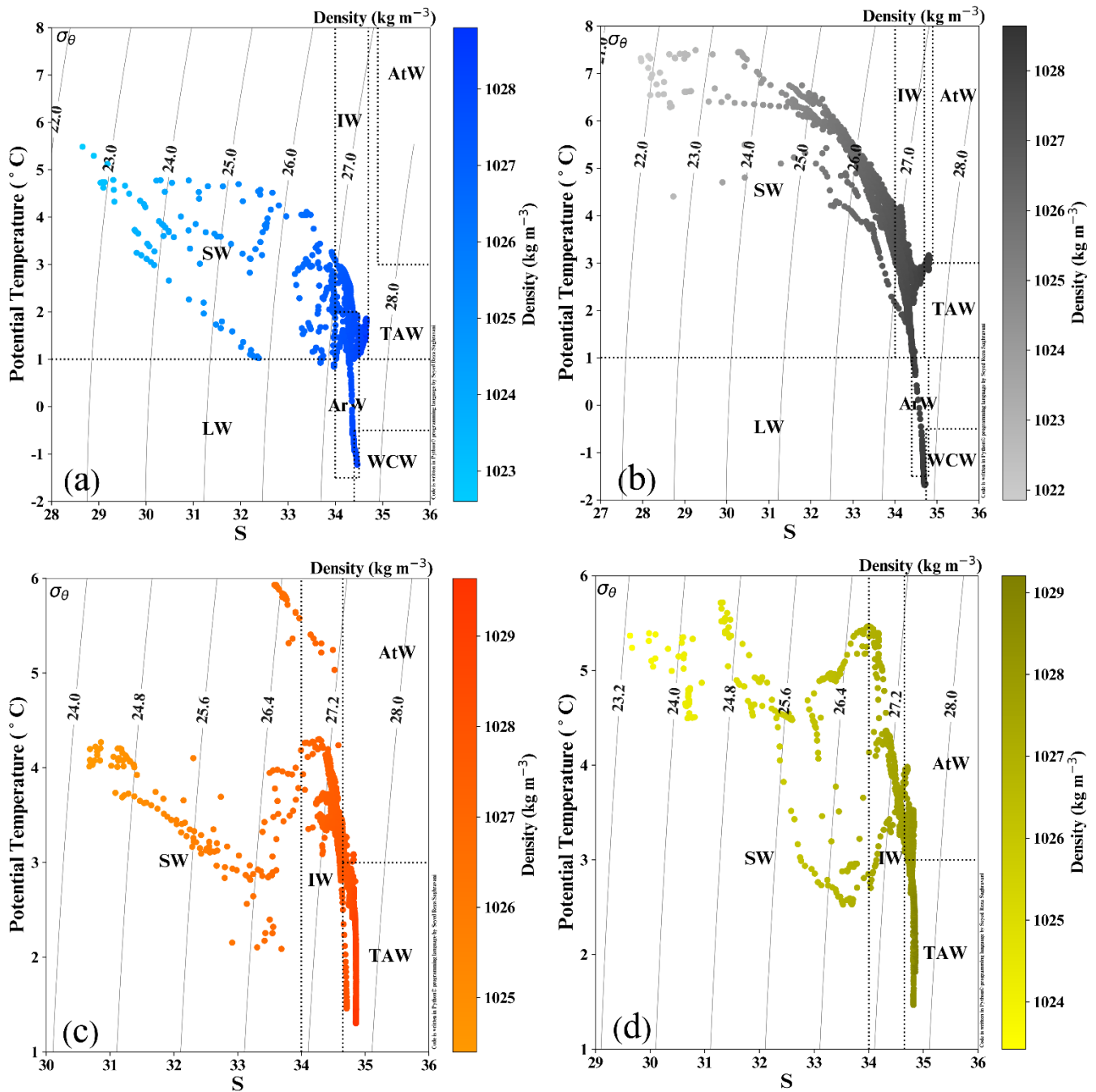
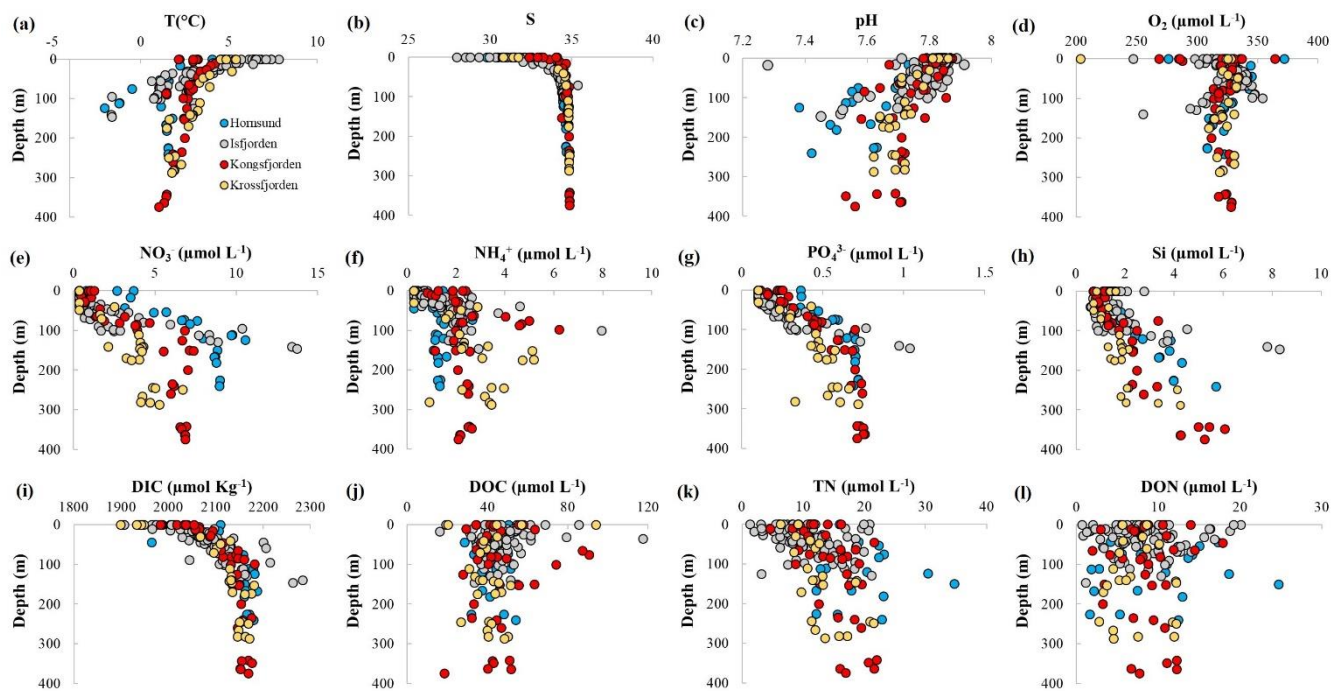


Fig.2 The water masses distribution such as surface water (SW), Arctic Water (ArW), Winter-Cooled Water (WCW), Intermediate Water (IW), Local Water (LW), Transformed Atlantic Water (TAW) and Atlantic Water (AtW) in a) Hornsund, b) Isfjorden, c) Kongsfjorden and d) Krossfjorden.



275 **Fig.3** Distribution of a) temperature (T), b) salinity (S), c) pH, d) oxygen (O_2), e) nitrate (NO_3^-), f) ammonium (NH_4^+), g) phosphate (PO_4^{3-}), h) dissolved silica (Si), i) dissolved inorganic carbon (DIC), j) dissolved organic carbon (DOC), k) total dissolved nitrogen (TN) and l) dissolved organic nitrogen (DON) in Hornsund (marked blue), Isfjorden (marked grey), Kongsfjorden (marked red) and Krossfjorden (marked yellow).

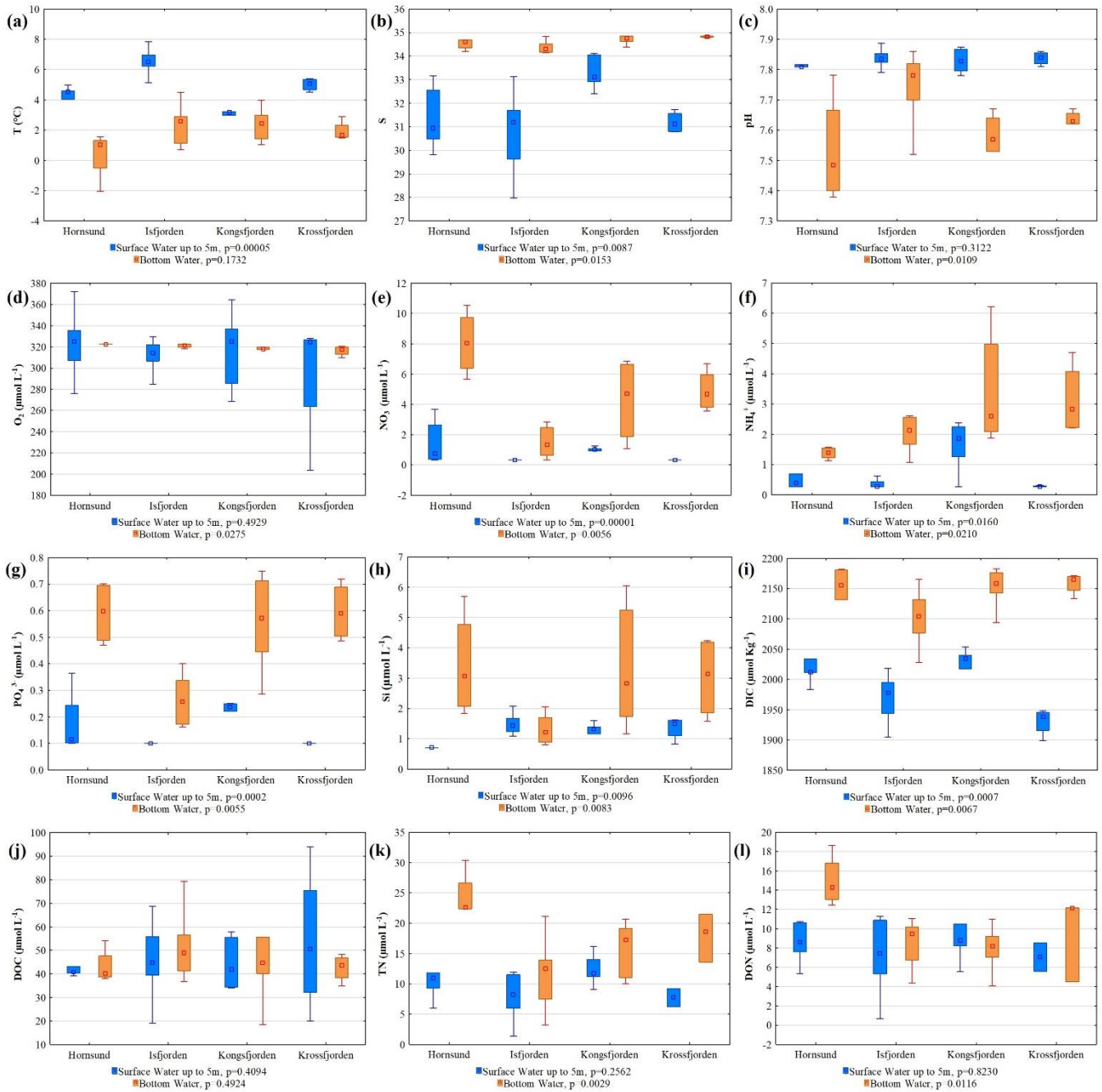


Fig.4 Box plots of a) temperature (T), b) salinity (S), c) pH, d) oxygen (O_2), e) nitrate (NO_3^-), f) ammonium (NH_4^+), g) phosphate (PO_4^{3-}), h) dissolved silica (Si), i) dissolved inorganic carbon (DIC), j) dissolved organic carbon (DOC), k) total dissolved nitrogen (TN) and l) dissolved organic nitrogen (DON) in surface water (marked blue) and bottom water (marked orange) in Hornsund, Isfjorden, Kongsfjorden and Krossfjorden. The p-values indicate significant differences in the median concentration of the parameter between the investigated fjords.

280

285

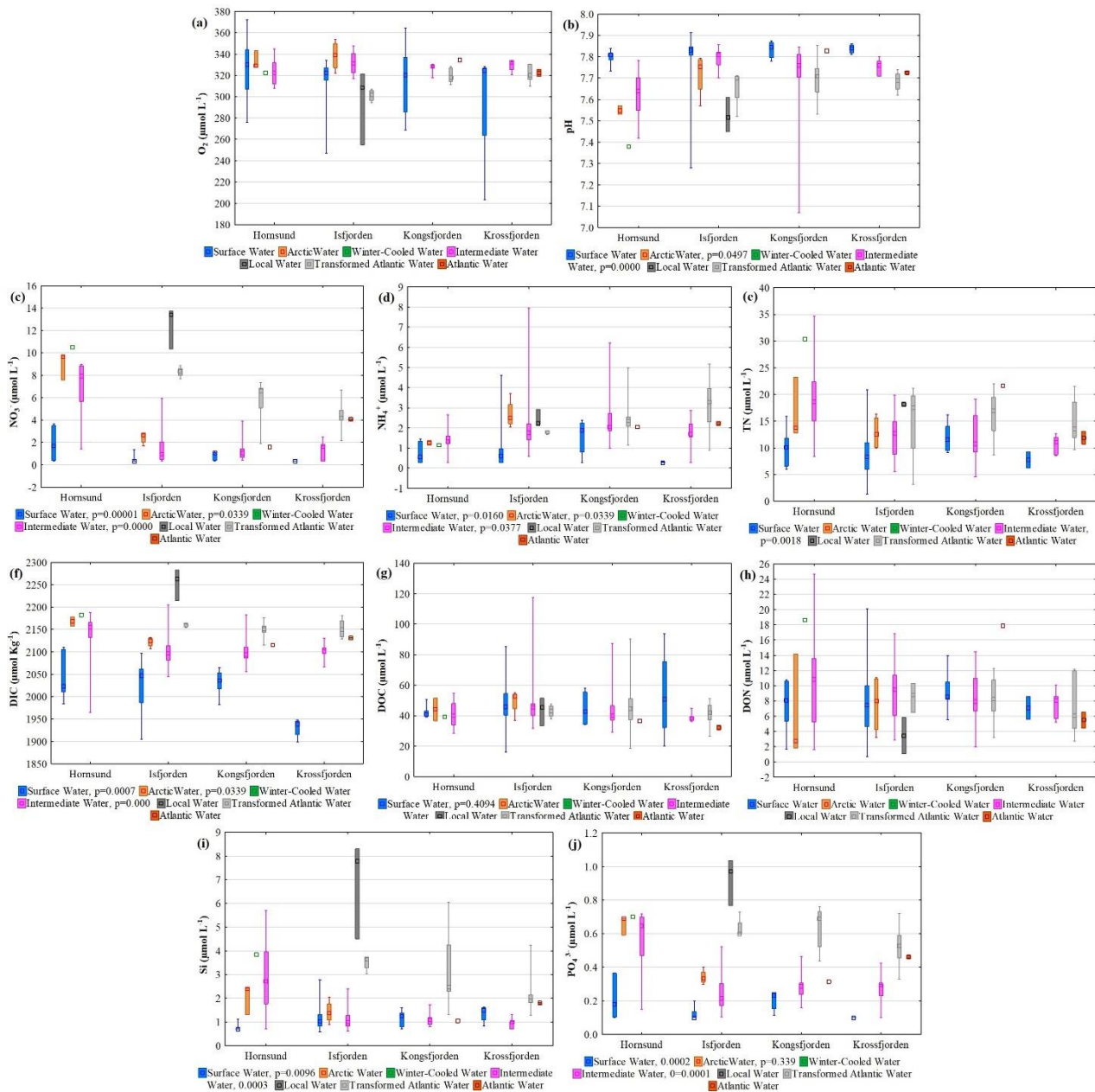


Fig.5 a) Oxygen (O_2), b) pH, c) nitrate (NO_3^-), d) ammonium (NH_4^+), e) total dissolved nitrogen (TN), f) dissolved inorganic carbon (DIC), g) dissolved organic carbon (DOC), h) dissolved organic nitrogen (DON), i) dissolved silica (Si), and j) phosphate (PO_4^{3-}) in surface water (marked as blue), Arctic Water (marked orange), Winter-Cooled Water (marked green), Intermediate Water (marked pink), Local Water (marked dark grey), Transformed Atlantic Water (marked light grey) and Atlantic Water (marked red) in Hornsund, Isfjorden, Kongsfjorden and Krossfjorden. The p-values indicate significant differences in the median concentration of the parameter between the investigated fjords, presented only if statistically significant.

290

295

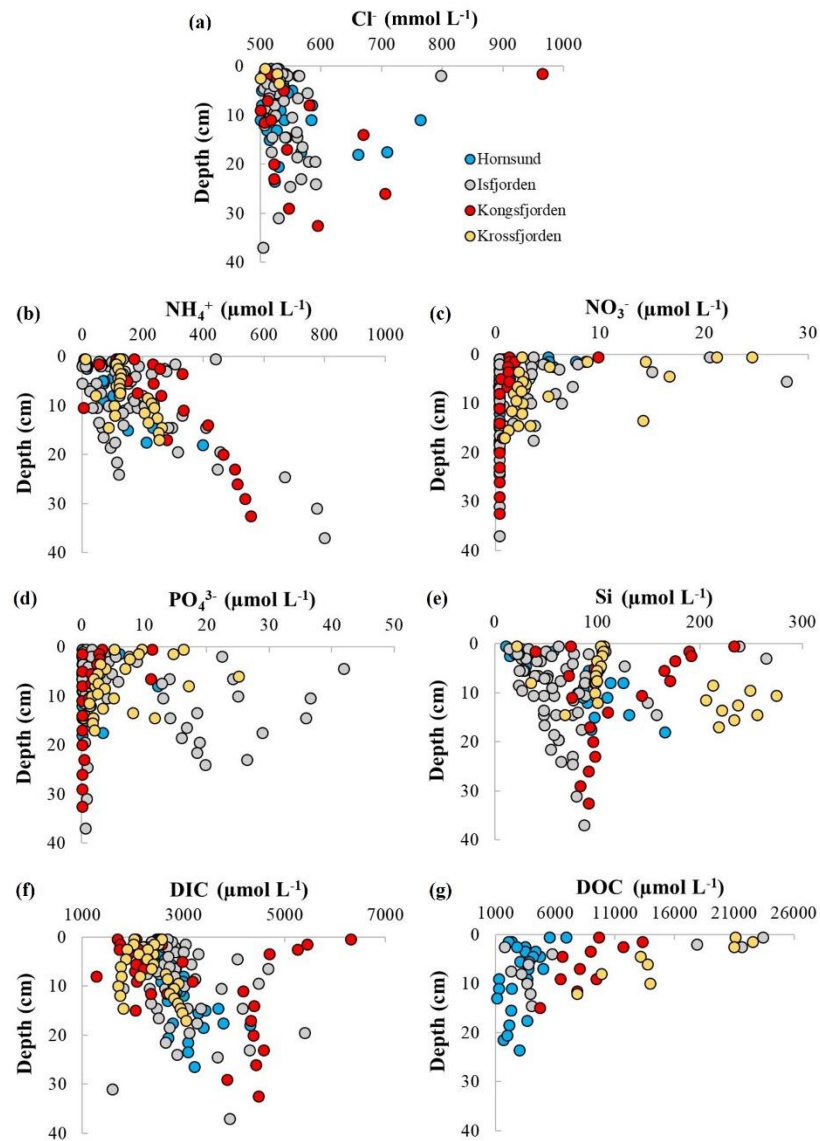


Fig.6 Distribution of a) chloride (Cl^-), b) ammonium (NH_4^+), c) nitrate (NO_3^-), d) phosphate (PO_4^{3-}), f) dissolved silica (Si), g) dissolved inorganic carbon (DIC), and h) dissolved organic carbon (DOC) in pore water in Hornsund (marked blue), Isfjorden (marked grey), Kongsfjorden (marked red) and Krossfjorden (marked yellow).

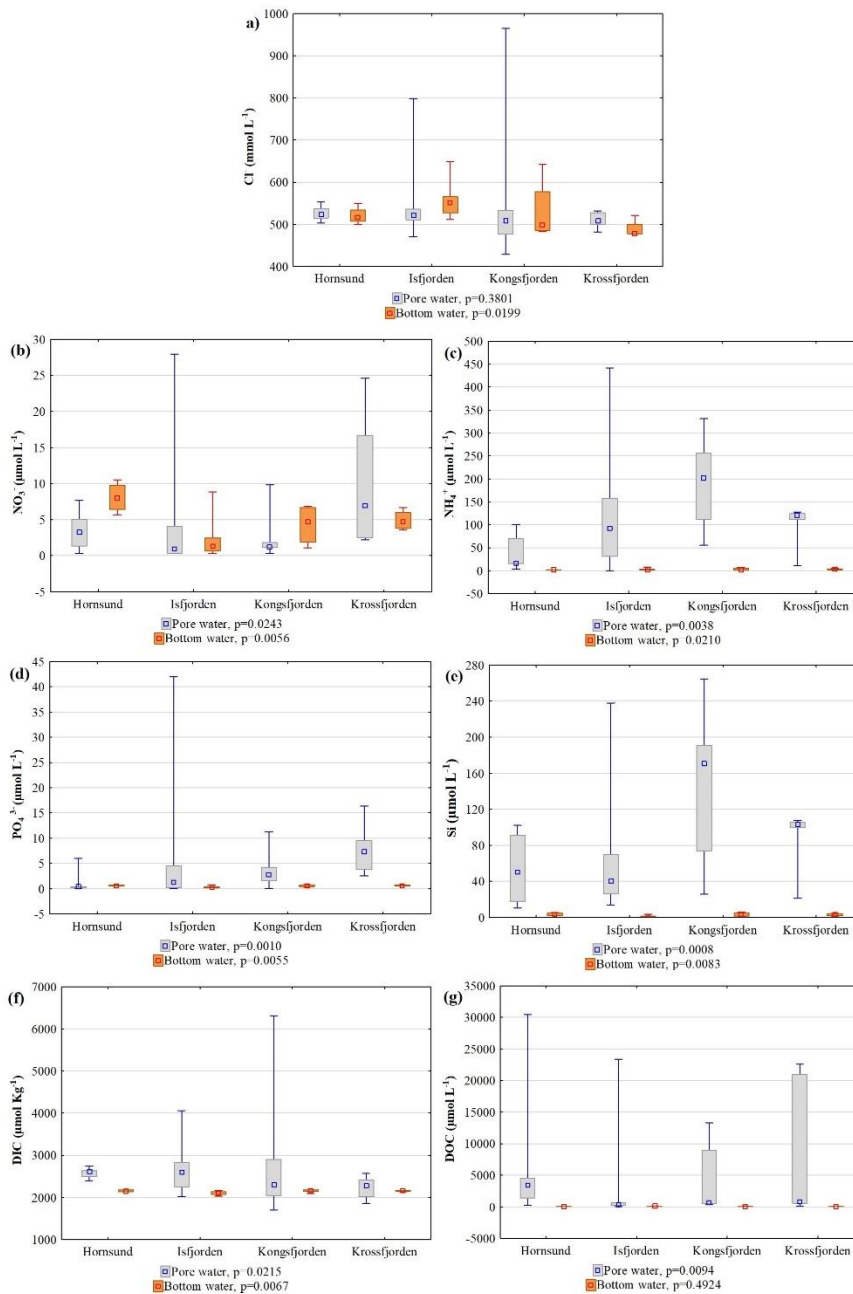


Fig.7 Box plots of a) chloride (Cl⁻), b) nitrate (NO₃⁻), c) ammonium (NH₄⁺), d) phosphate (PO₄³⁻), e) dissolved silica (Si), f) dissolved inorganic carbon (DIC), and g) dissolved organic carbon (DOC) in pore water (marked grey) and bottom water (marked orange) in Hornsund, Isfjorden, Kongsfjorden and Krossfjorden. The p-values indicate significant differences in the median concentration of the parameter between the investigated fjords.

Author contributions

SRS: Conceptualization, data interpretation, preparation of figures, investigation, writing—original draft, reviewing and editing.
MB, WH, KK, AL, AS, BSz: Reviewing and editing.

310 Competing interests

The contact author has declared that none of the authors has any competing interests.

Acknowledgments

We thank our colleagues (Przemysław Makuch, Magdalena Diak, Marta Borecka, Katarzyna Koziarowska- Makuch, Fernando
315 Aquado Gonzalo, Marcin Stokowski, Aleksandra Winogradow, Miłosz Grabowski, and Marek Zajączkowski) for sharing ideas
and for help with field and laboratory work. We would like to acknowledge Laura Bromboszcz and Piotr Prusiński for their
technical support. We would like to thank the captain and the crew of r/v OCEANIA. CTD data were collected and processed
at the Observational Oceanography Laboratory under the AREX monitoring program as a contribution to statutory research
areas (task I.4).

320

Financial support

The authors declare financial support was received for the research, authorship, and/or publication of this article. The research
leading to these results has received funding from the Norwegian Financial Mechanism 2014–2021 project no.
2019/34/H/ST10/00645 and 2019/34/H/ST10/00504. In addition, the present study is financed by statutory activities of the
325 Institute of Oceanology Polish Academy of Science and National Science Centre project no. 2019/34/E/ST10/00167.

References

- Cantoni, C., Hopwood, M. J., Clarke, J. S., Chiggiato, J., Achterberg, E. P., and Cozzi, S.: Glacial Drivers of Marine
Biogeochemistry Indicate a Future Shift to More Corrosive Conditions in an Arctic Fjord, *J. Geophys. Res. Biogeosciences*,
330 125, <https://doi.org/10.1029/2020JG005633>, 2020.
- Codispoti, L. A., Kelly, V., Thessen, A., Matrai, P., Suttles, S., Hill, V., Steele, M., and Light, B.: Synthesis of primary
production in the Arctic Ocean: III. Nitrate and phosphate based estimates of net community production, *Prog. Oceanogr.*,
110, 126–150, <https://doi.org/10.1016/j.pocean.2012.11.006>, 2013.
- Cottier, F., Tverberg, V., Inall, M., Svendsen, H., Nilsen, F., and Griffiths, C.: Water mass modification in an Arctic fjord
335 through cross-shelf exchange: The seasonal hydrography of Kongsfjorden, Svalbard, *J. Geophys. Res. Ocean.*, 110, 1–18,
<https://doi.org/10.1029/2004JC002757>, 2005.
- Drewnik, A., Węsławski, J. M., Włodarska-Kowalczyk, M., Łącka, M., Promińska, A., Zaborska, A., and Gluchowska, M.:
From the worm’s point of view. I: Environmental settings of benthic ecosystems in Arctic fjord (Hornsund, Spitsbergen), *Polar
Biol.*, 39, 1411–1424, <https://doi.org/10.1007/s00300-015-1867-9>, 2016.

- 340 Dunse, T., Dong, K., Aas, K. S., and Stige, L. C.: Regional-scale phytoplankton dynamics and their association with glacier meltwater runoff in Svalbard, *Biogeosciences*, 19, 271–294, <https://doi.org/10.5194/bg-19-271-2022>, 2022.
- Finne, E. A., Varpe, Ø., Durant, J. M., Gabrielsen, G. W., and Poste, A. E.: Nutrient fluxes from an Arctic seabird colony to the adjacent coastal marine ecosystem, *Polar Biol.*, <https://doi.org/10.1007/s00300-022-03024-5>, 2022.
- Gamboa-Sojo, V. M., Husum, K., Morigi, C., Divine, D., and Miettinen, A.: Environmental changes in Krossfjorden, Svalbard, since 1950: Benthic foraminiferal and stable isotope evidence, *Arctic, Antarct. Alp. Res.*, 54, 465–477, <https://doi.org/10.1080/15230430.2022.2120246>, 2022.
- 345 Grabiec, M., Ignatiuk, D., Jania, J. A., Moskalik, M., Głowacki, P., Błaszczuk, M., Budzik, T., and Walczowski, W.: Coast formation in an Arctic area due to glacier surge and retreat: The Hornbreen-Hambergreen case from Spistbergen, *Earth Surf. Process. Landforms*, 43, 387–400, <https://doi.org/10.1002/esp.4251>, 2018.
- 350 Grasshoff, K., Erhardt, M., Kremling, K. (Eds.), 1983. *Methods of seawater analysis*. Verlag Chemie, Germany, 419 pp., <https://doi.org/10.1002/iroh.19850700232>.
- Gundersen, K., Møgster, J. S., Lien, V. S., Ershova, E., Lunde, L. F., Arnesen, H., and Olsen, A.-K.: Thirty Years of Nutrient Biogeochemistry in the Barents Sea and the adjoining Arctic Ocean, 1990–2019, *Sci. Data*, 9, 649, <https://doi.org/10.1038/s41597-022-01781-w>, 2022.
- 355 Halbach, L., Vihtakari, M., Duarte, P., Everett, A., Granskog, M. A., Hop, H., Kauko, H. M., Kristiansen, S., Myhre, P. I., Pavlov, A. K., Pramanik, A., Tatarek, A., Torsvik, T., Wiktor, J. M., Wold, A., Wulff, A., Steen, H., and Assmy, P.: Tidewater Glaciers and Bedrock Characteristics Control the Phytoplankton Growth Environment in a Fjord in the Arctic, *Front. Mar. Sci.*, 6, 1–18, <https://doi.org/10.3389/fmars.2019.00254>, 2019.
- Henley, S. F., Porter, M., Hobbs, L., Braun, J., Guillaume-Castel, R., Venables, E. J., Dumont, E., and Cottier, F.: Nitrate supply and uptake in the Atlantic Arctic sea ice zone: seasonal cycle, mechanisms and drivers, *Philos. Trans. R. Soc. A Math. Phys. Eng. Sci.*, 378, 20190361, <https://doi.org/10.1098/rsta.2019.0361>, 2020.
- Hodal, H., Falk-Petersen, S., Hop, H., Kristiansen, S., and Reigstad, M.: Spring bloom dynamics in Kongsfjorden, Svalbard: Nutrients, phytoplankton, protozoans and primary production, *Polar Biol.*, 35, 191–203, <https://doi.org/10.1007/s00300-011-1053-7>, 2012.
- 365 Hop, H. and Wiencke, C.: The Ecosystem of Kongsfjorden, Svalbard, 1–20, https://doi.org/10.1007/978-3-319-46425-1_1, 2019.
- Hop, H., Falk-Petersen, S., Svendsen, H., Kwasniewski, S., Pavlov, V., Pavlova, O., and Søreide, J. E.: Physical and biological characteristics of the pelagic system across Fram Strait to Kongsfjorden, *Prog. Oceanogr.*, 71, 182–231, <https://doi.org/10.1016/j.pocean.2006.09.007>, 2006.
- 370 Hopwood, M. J., Connelly, D. P., Arendt, K. E., Juul-Pedersen, T., Stinchcombe, M. C., Meire, L., Esposito, M., and Krishna, R.: Seasonal Changes in Fe along a Glaciated Greenlandic Fjord, *Front. Earth Sci.*, 4, <https://doi.org/10.3389/feart.2016.00015>, 2016.

- Hopwood, M. J., Carroll, D., Dunse, T., Hodson, A., Holding, J. M., Iriarte, J. L., Ribeiro, S., Achterberg, E. P., Cantoni, C., Carlson, D. F., Chierici, M., Clarke, J. S., Cozzi, S., Fransson, A., Juul-Pedersen, T., Winding, M. H. S., and Meire, L.: Review article: How does glacier discharge affect marine biogeochemistry and primary production in the Arctic?, *Cryosph.*, 14, 1347–1383, <https://doi.org/10.5194/tc-14-1347-2020>, 2020.
- Intergovernmental Panel on Climate Change (IPCC): *The Ocean and Cryosphere in a Changing Climate*, Cambridge University Press, 203–320 pp., <https://doi.org/10.1017/9781009157964>, 2022.
- Kelley, D. E.: *Oceanographic Analysis with R*, <https://doi.org/10.1007/978-1-4939-8844-0>, 2018.
- 375 Kim, J. H., Ryu, J. S., Hong, W. L., Jang, K., Joo, Y. J., Lemarchand, D., Hur, J., Park, M. H., Chen, M., Kang, M. H., Park, S., Nam, S. Il, and Lee, Y. K.: Assessing the impact of freshwater discharge on the fluid chemistry in the Svalbard fjords, *Sci. Total Environ.*, 835, 155516, <https://doi.org/10.1016/j.scitotenv.2022.155516>, 2022.
- 380 Ko, E., Gorbunov, M. Y., Jung, J., Joo, H. M., Lee, Y., Cho, K., Yang, E. J., Kang, S., and Park, J.: Effects of Nitrogen Limitation on Phytoplankton Physiology in the Western Arctic Ocean in Summer, *J. Geophys. Res. Ocean.*, 125, <https://doi.org/10.1029/2020JC016501>, 2020.
- 385 Laufer-Meiser, K., Michaud, A. B., Maisch, M., Byrne, J. M., Kappler, A., Patterson, M. O., Røy, H., and Jørgensen, B. B.: Potentially bioavailable iron produced through benthic cycling in glaciated Arctic fjords of Svalbard, <https://doi.org/10.1038/s41467-021-21558-w>, 2021.
- McGovern, M., Pavlov, A. K., Deininger, A., Granskog, M. A., Leu, E., Søreide, J. E., and Poste, A. E.: Terrestrial Inputs Drive Seasonality in Organic Matter and Nutrient Biogeochemistry in a High Arctic Fjord System (Isfjorden, Svalbard), *Front. Mar. Sci.*, 7, 1–15, <https://doi.org/10.3389/fmars.2020.542563>, 2020.
- 390 Menze, S., Ingvaldsen, R. B., Nikolopoulos, A., Hattermann, T., Albrechtsen, J., and Gjørseter, H.: Productive detours – Atlantic water inflow and acoustic backscatter in the major troughs along the Svalbard shelf, *Prog. Oceanogr.*, 188, 102447, <https://doi.org/10.1016/j.pocean.2020.102447>, 2020.
- 395 Mills, M. M., Brown, Z. W., Laney, S. R., Ortega-Retuerta, E., Lowry, K. E., van Dijken, G. L., and Arrigo, K. R.: Nitrogen Limitation of the Summer Phytoplankton and Heterotrophic Prokaryote Communities in the Chukchi Sea, *Front. Mar. Sci.*, 5, <https://doi.org/10.3389/fmars.2018.00362>, 2018.
- Moskalik, M., Tęgowski, J., Grabowiecki, P., and Żulichowska, M.: Principal Component and Cluster Analysis for determining diversification of bottom morphology based on bathymetric profiles from Brepollen (Hornsund, Spitsbergen)**The project was partly supported by The Polish Ministry of Sciences and Higher Education Gr, *Oceanologia*, 56, 59–84, <https://doi.org/10.5697/oc.56-1.059>, 2014.
- 400 Nilsen, F., Cottier, F., Skogseth, R., and Mattsson, S.: Fjord-shelf exchanges controlled by ice and brine production: The interannual variation of Atlantic Water in Isfjorden, Svalbard, *Cont. Shelf Res.*, 28, 1838–1853, <https://doi.org/10.1016/j.csr.2008.04.015>, 2008.
- 405 Pavlova, O., Gerland, S., and Hop, H.: Changes in Sea-Ice Extent and Thickness in Kongsfjorden, Svalbard (2003–2016), 105–136, https://doi.org/10.1007/978-3-319-46425-1_4, 2019.

- Pogojeva, M., Polukhin, A., Makkaveev, P., Staalstrøm, A., Berezina, A., and Yakushev, E.: Arctic Inshore Biogeochemical Regime Influenced by Coastal Runoff and Glacial Melting (Case Study for the Templefjord, Spitsbergen), *Geosci.*, 12, <https://doi.org/10.3390/geosciences12010044>, 2022.
- 410 Promińska, A., Cisek, M., and Walczowski, W.: Kongsfjorden and Hornsund hydrography – comparative study based on a multiyear survey in fjords of west Spitsbergen, *Oceanologia*, 59, 397–412, <https://doi.org/10.1016/j.oceano.2017.07.003>, 2017.
- Promińska, A., Falck, E., and Walczowski, W.: Interannual variability in hydrography and water mass distribution in Hornsund, an Arctic fjord in Svalbard, *Polar Res.*, 37, <https://doi.org/10.1080/17518369.2018.1495546>, 2018.
- Rudels, B., R. Meyer, E. Fahrbach, V. Ivanov, S. Osterhus, D. Quadfasel, U. Schauer, V. Tverburg, and R. A. Woodgate, The
415 water mass distribution in Fram Strait and over the Yermak Plateau in summer 1997, *Ann. Geophys.*, 18, 687–705, 2000.
- Santos-Garcia, M., Ganeshram, R. S., Tuerena, R. E., Debyser, M. C. F., Husum, K., Assmy, P., and Hop, H.: Nitrate isotope investigations reveal future impacts of climate change on nitrogen inputs and cycling in Arctic fjords: Kongsfjorden and Rijpfjorden (Svalbard), *Biogeosciences*, 19, 5973–6002, <https://doi.org/10.5194/bg-19-5973-2022>, 2022.
- Schlegel, R., Bartsch, I., Bischof, K., Bjørst, L. R., Dannevig, H., Diehl, N., Duarte, P., Hovelsrud, G. K., Juul-Pedersen, T.,
420 Lebrun, A., Merillet, L., Miller, C., Ren, C., Sejr, M., Søreide, J. E., Vonnahme, T. R., and Gattuso, J.-P.: Drivers of change in Arctic fjord socio-ecological systems: Examples from the European Arctic, *Cambridge Prism. Coast. Futur.*, 1, e13, <https://doi.org/10.1017/cft.2023.1>, 2023.
- Singh, A. and Krishnan, K. P.: The spatial distribution of phytoplankton pigments in the surface sediments of the Kongsfjorden and Krossfjorden ecosystem of Svalbard, Arctic, Reg. Stud. Mar. Sci., 31, 100815,
425 <https://doi.org/10.1016/j.rsma.2019.100815>, 2019.
- Smola, Z. T., Tatarek, A., Wiktor, J. M., Wiktor, J. M. W., Kubiszyn, A., and Węśławski, J. M.: Primary producers and production in Hornsund and Kongsfjorden - Comparison of two fjord systems, *Polish Polar Res.*, 38, 351–373, <https://doi.org/10.1515/popore-2017-0013>, 2017.
- Stroeve, J., Vancoppenolle, M., Veyssiere, G., Lebrun, M., Castellani, G., Babin, M., Karcher, M., Landy, J., Liston, G. E.,
430 and Wilkinson, J.: A Multi-Sensor and Modeling Approach for Mapping Light Under Sea Ice During the Ice-Growth Season, *Front. Mar. Sci.*, 7, 1–28, <https://doi.org/10.3389/fmars.2020.592337>, 2021.
- Svendsen, H., Beszczynska-Møller, A., Hagen, J. O., Lefauconnier, B., Tverberg, V., Gerland, S., Ørbøk, J. B., Bischof, K., Papucci, C., Zajaczkowski, M., Azzolini, R., Bruland, O., Wiencke, C., Winther, J. G., and Dallmann, W.: The physical environment of Kongsfjorden-Krossfjorden, and Arctic fjord system in Svalbard, *Polar Res.*, 21, 133–166,
435 <https://doi.org/10.1111/j.1751-8369.2002.tb00072.x>, 2002.
- Svendsen, J. I., Mangerud, J., Elverhøi, A., Solheim, A., and Schüttenhelm, R. T. E.: The Late Weichselian glacial maximum on western Spitsbergen inferred from offshore sediment cores, *Mar. Geol.*, 104, 1–17, [https://doi.org/10.1016/0025-3227\(92\)90081-R](https://doi.org/10.1016/0025-3227(92)90081-R), 1992.

- Szymczycha, B., Saghravani, S. R., Böttcher, M. E., Hong, W.-L., Kuliński, K., Lepland, A., and Sen, A.: In-situ parameters, nutrients and dissolved carbon distribution in the water column and pore waters of Arctic Fjords (Western Spitsbergen) during a melting season, <https://doi.org/10.5281/zenodo.11237340>, 2024.
- Townhill, B. L., Reppas-Chrysovitsinos, E., Sühling, R., Halsall, C. J., Mengo, E., Sanders, T., Dähnke, K., Crabeck, O., Kaiser, J., and Birchenough, S. N. R.: Pollution in the Arctic Ocean: An overview of multiple pressures and implications for ecosystem services, *Ambio*, 51, 471–483, <https://doi.org/10.1007/s13280-021-01657-0>, 2022.
- 445 Tuerena, R. E., Mahaffey, C., Henley, S. F., de la Vega, C., Norman, L., Brand, T., Sanders, T., Debyser, M., Dähnke, K., Braun, J., and März, C.: Nutrient pathways and their susceptibility to past and future change in the Eurasian Arctic Ocean, *Ambio*, 51, 355–369, <https://doi.org/10.1007/s13280-021-01673-0>, 2022.
- Vihtakari, M., 2022. ggOceanMaps: plot data on oceanographic maps using “ggplot2”. R package version 1.2. 6.
- Vihtakari, M., 2020. PlotSvalbard: PlotSvalbard - Plot research data from Svalbard on maps.
- 450 Włodarska-Kowalczyk, M., Węśławski, J. M., and Kotwicki, L.: Spitsbergen glacial bays macrobenthos - a comparative study, *Polar Biol.*, 20, 66–73, <https://doi.org/10.1007/s003000050277>, 1998.
- Zaborska, A., Strzelewicz, A., Rudnicka, P., and Moskalik, M.: Processes driving heavy metal distribution in the seawater of an Arctic fjord (Hornsund, southern Spitsbergen), *Mar. Pollut. Bull.*, 161, 111719, <https://doi.org/10.1016/j.marpolbul.2020.111719>, 2020.

455